

The Non-Parametric Model for Linking Galaxy Luminosity with Halo/Subhalo Mass

A. Vale^{1*} and J. P. Ostriker^{1,2}

¹*Institute of Astronomy, University of Cambridge, Madingley Road, Cambridge CB3 0HA, United Kingdom*

²*Princeton University Observatory, Princeton University, Princeton NJ 08544, USA*

Accepted..... Received.....; in original form 30 November 2005

ABSTRACT

Non-parametric, empirically based, models for associating galaxy luminosities with halo/subhalo masses are being developed by several groups and we present here an updated version of the Vale & Ostriker (2004) version of this model. This is based on a more accurate, self-consistent treatment of subhalo mass loss and revised results for the subhalo mass function to address this question anew. We find that the mass-luminosity relation, at high mass, particularly for first brightest galaxies and less so for group total, is almost independent of the actual luminosity function considered, when luminosity is scaled by the characteristic luminosity L_* . Additionally, the shape of the total luminosity depends on the slope of the subhalo mass function. For these high mass, cluster sized haloes we find that total luminosity scales as $L_{tot} \sim M^{0.88}$, while the luminosity of the first brightest galaxy has a much weaker dependence on halo mass, $L_1 \sim M^{0.28}$, in good agreement with observations and previous results. At low mass, the resulting slope of the mass luminosity relation depends strongly of the faint end slope of the luminosity function, and we obtain a steep relation, with approximately $L \sim M^{4.5}$ for $M \sim 10^{10} h^{-1} M_\odot$ in the K-band. The average number of galaxies per halo/cluster is also in very good agreement with observations, scaling as $\sim M^{0.9}$.

In general, we obtain a good agreement with several independent sets of observational data. Taking the model as essentially correct, we consider two additional possible sources for remaining discrepancies: problems with the underlying cosmology and with the observational mass determination. We find that, when comparing with observations and for a flat cosmology, the model tends to prefer lower values for Ω_m and σ_8 . Within the WMAP+SDSS concordance plane of Tegmark et al. (2004), we find best agreement around $\Omega_m = 0.25$ and $\sigma_8 = 0.8$; this is also in very good agreement with the results of the CMB+2dF study of Sanchez et al. (2005). We also check on possible corrections for observed mass based on a comparison of the equivalent number of haloes/clusters. Additionally, we include further checks on the model results based on the mass to light ratio, the occupation number, the group luminosity function and the multiplicity function.

Key words: galaxies: haloes – cosmology: theory – dark matter – large-scale structure of the universe

1 INTRODUCTION

One of the outstanding challenges of cosmology is to relate the more theoretical aspect of the standard cosmological model, in the form of the large scale distribution of dark matter as seen in high resolution N-body simulations, to the observational evidence, as reflected by large galaxy sur-

veys. Or, in a directly related question, what is the relation between observable properties of galaxies and computable properties of dark matter haloes?

The traditional route to looking at this problem has been to follow the theory of galaxy formation. This can be tested through the results of hydrodynamical simulations (White, Hernquist, & Springel 2001; Yoshikawa et al. 2001; Pearce et al. 2001; Nagamine et al. 2001; Berlind et al. 2003; Meza et al. 2003; Bailin et al. 2005), which combine

* E-mail: avale@ast.cam.ac.uk

dark matter with baryons, or semi-analytical models of galaxy formation (Kauffmann, Nusser, & Steinmetz 1997; Governato et al. 1998; Kauffmann et al. 1999a,b; Benson et al. 2000a,b; Sheth & Diaferio 2001; Somerville et al. 2001; Wechsler et al. 2001; Benson et al. 2003; Berlind et al. 2003). This is a powerful way of looking at the problem, since it provides a direct answer, and a galaxy formation theory is an end goal in itself. There are, however, some problems: first and foremost, the theory behind galaxy formation has several components which are ill understood, and where the best approach remains phenomenological. At the same time, the required very high resolution, large scale, full hydrodynamical simulations including magnetic fields and radiative transfer are beyond current computing resources.

In the past few years, a new approach has appeared which is in many ways an alternative: this consists of an indirect method, associating galaxy and dark matter halo properties in an empirical manner. This is usually done through a statistical approach, either by focusing directly on the number of galaxies in each halo, as is done in halo occupation distribution models (Seljak 2000; Benson 2001; Bullock, Wechsler, & Somerville 2002; Zheng et al. 2002; Berlind & Weinberg 2002; Berlind et al. 2003; Magliocchetti & Porciani 2003), or through the luminosity distribution of the galaxies in a halo, like the conditional luminosity function approach (van den Bosch, Yang & Mo 2003; Yang, Mo & van den Bosch 2003; van den Bosch et al. 2005; Cooray & Milosavljević 2005b; Cooray 2005a,b), or finally by building a direct relation between mass and luminosity (Peacock & Smith 2000; Kravtsov et al. 2004; Vale & Ostriker 2004; Tasitsiomi et al. 2004).

In the present paper, we take the latter approach. We use new, high resolution simulation results for the subhalo mass distribution, together with a self consistent approximation to subhalo mass loss, to build the total distribution of dark matter hosts based on physical theory. Together with the empirically determined galaxy luminosity function, this yields a mass luminosity relation for an individual galaxy and the halo or subhalo which hosts it. This is in part an updated version of the preliminary model shown in Vale & Ostriker (2004, hereafter paper I).

This paper is organised as follows: in section 2, we introduce the non-parametric model and the main concepts behind it. In section 3, we look in some detail at the subhalo mass function, introducing a prescription for subhalo mass loss and in particular looking at how to define this mass function in terms of the original, pre-merger into parent, mass of the subhaloes. In section 4, we give the main results for our base model, using the K-band luminosity function from the 2MASS survey. In section 5, we look at how the model results change depending on the luminosity function (and hence waveband) used, as well as the effect of changing the underlying cosmological model and what we find is the most relevant parameter of the subhalo mass function, the low mass slope. We also look at potential problems with the observational mass determination. We present additional checks of the model in section 6, by calculating the predicted mass to light ratio, occupation number, group luminosity function and multiplicity function. Finally, we conclude in section 7.

2 THE NON-PARAMETRIC MODEL

The basic idea behind the non-parametric model is to assume a monotonic and one to one relation between the luminosity of a galaxy and the mass of the dark matter halo or subhalo which hosts it. This comes from the standard picture that galaxies are formed in haloes through the accretion of gas, the amount of which is a monotonic function of the depth of the potential well of the halo and thus of its mass. By including the subhaloes, we are assuming that all galaxies are either hosted individually in a parent halo, or in the case of multiple systems like clusters in one of the subhaloes. In fact, we assume that counting haloes and subhaloes accounts for all hosts, and exclude complications such as conditions during ongoing mergers. Groups and clusters are then formed when haloes merge; the end result of such a build up is to have a central galaxy, which formed in the most massive of the initial haloes (which subsequently became the parent), and satellite galaxies in the smallest haloes which were accreted and which became subhaloes.

Using this basic concept, it becomes possible to obtain an average relation between the luminosity of a galaxy and its host halo/subhalo mass by matching the numbers of each, the former from large scale galaxy surveys, the latter from dark matter simulations. The average luminosity L of a galaxy in a halo or subhalo of mass M will then simply be given by:

$$\int_L^\infty \phi(L)dL = \int_M^\infty n(M)dM, \quad (1)$$

where $\phi(L)$ is the galaxy luminosity function and $n(M) = n_H(M) + n_{SH}(M)$ is the sum of the halo and subhalo mass functions.

During and after the halo merging process significant star formation in the subhalo declines (e.g., Kauffmann, White & Guiderdoni 1993; Somerville & Primack 1999; Cole et al. 2000), so we will take as a constraint that the amount of gas accreted by what becomes a subhalo, and which will thus be available to form a satellite galaxy, will be proportional not to the mass it has at present, but to the maximum mass it had before being accreted by its parent halo and undergoing mass loss to tidal stripping and dynamical friction. This is supported by some recent work of Libeskind et al. (2005), who use high resolution N-body simulations together with semi-analytical modelling of the formation of galaxies to study the distribution of satellites in Milky Way type galaxies. They find that while the spatial distribution of satellite galaxies is significantly different from that of the most massive present day subhaloes, it is well matched by that of the subset of subhaloes with the most massive progenitors. It is then necessary to use not the distribution of subhaloes as a function of their present mass, but instead of the original mass they had prior to accretion into the parent and subsequent mass loss, regardless of theoretical issues related to galaxy formation. We circumvent this problem by coupling the present, evolved subhalo mass function with a prescription for the amount of mass loss, together with some simple arguments on the total mass contained in these subhalo progenitors, in order to regain the initial mass of a subhalo at the moment of accretion and tag each of these by its initial mass.

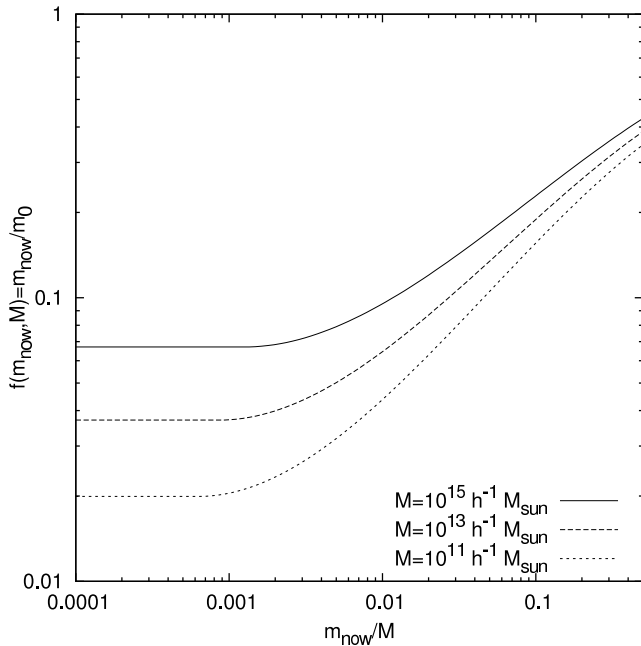


Figure 1. Mass loss factor $f(m_{\text{now}}/m_0)$, which is a function both of subhalo and parent halo mass. Plotted are curves for three different parent halo masses, $10^{15}h^{-1}M_{\odot}$, $10^{13}h^{-1}M_{\odot}$, $10^{11}h^{-1}M_{\odot}$, from top to bottom respectively. These curves have the normalization we obtained directly from adopting the results of van den Bosch, Tormen & Giocoli (2005); it may be necessary to renormalize them when considering different present subhalo mass functions (see text for discussion).

3 SUBHALOES

3.1 Mass loss

As discussed, the first step to having a workable non-parametric model is to account for the amount of mass loss in subhaloes. To obtain it, we adapt the results of van den Bosch, Tormen & Giocoli (2005), by comparing the results they give for the evolved and unevolved (original) subhalo mass functions. If we assume that the present and original masses of the subhaloes are related monotonically (that is, that the most massive of the original subhaloes are still the most massive at present, independently of the actual amount of mass loss), we can obtain this relation by comparing the total numbers of present subhaloes to their original progenitors, in a manner similar to the process presented above for the non-parametric model.

The resulting mass loss factors will depend on both the subhalo mass and the mass of the parent halo, as can be seen in figure 1. In fact, we have made a small further change to the results we obtain from the mass functions of van den Bosch, Tormen & Giocoli (2005), which is to flatten the mass loss factor to a constant at its minimum and so maintain monotonicity. The upturn at high subhalo mass is explained by two competing factors which contribute to mass loss: while the more massive subhaloes lose a larger fraction of their mass in each orbit within the parent halo, they will also, on average, have formed and therefore been accreted later, which means they will have undergone fewer of these orbits than less massive subhaloes (see for example, van den Bosch, Tormen & Giocoli 2005).

We can now apply this mass loss factor to subhalo mass functions measured from simulation results to obtain the original subhalo mass function. There is an important further consideration, though: care must be taken with the normalization of this function. In fact, we know that the sum of the mass in these original subhaloes must equal the total present mass in the parent halo, since the latter is built up by accreting and stripping subhaloes (ignoring for simplicity the small amount of mass associated with subhaloes that disappear totally). Therefore, when using different subhalo mass functions, the result presented in figure 1 should be taken only to be the shape of the mass loss factor. It is then necessary to either renormalize the mass loss factor (or alternatively the derived original subhalo mass function) to ensure that the total mass in these original subhaloes matches the present mass of the parent halo.

3.2 The subhalo mass function

The distribution of the subhaloes is based on the subhalo mass function (SHMF), $N(m|M)dm$, which gives the number of subhaloes in the mass range m to $m+dm$ for a parent halo of mass M . We start by defining the present day mass fraction in subhaloes as:

$$\gamma(M) \equiv \frac{1}{M} \int_0^{m_{\text{cut}}} mN(m|M)dm, \quad (2)$$

where $m_{\text{cut}}(M)$ is the mass of the most massive subhalo possible, which we take to be a function of the parent halo mass. This value will be set by assuming that the maximum original mass is half the total mass of the parent, $M/2$. This is in fact a question of definition, since a subhalo which had a mass greater than this would actually be larger than any other it could be merging with, and would itself in fact be the parent halo. This can be converted back to m_{cut} by using the mass loss factor.

This mass fraction in subhaloes is generally found to be a growing function of parent halo mass, both in simulations or semi-analytical models (e.g., Gao et al. 2004; van den Bosch, Tormen & Giocoli 2005; Shaw et al. 2005). As pointed out in van den Bosch, Tormen & Giocoli (2005), this is naturally due to the later formation of more massive haloes, therefore allowing less time for mass loss to occur. There also seems to be some agreement that the value of this mass fraction should be just under 10%, even at high halo mass. This will have as an important consequence that the subhalo mass function cannot possibly be universal but must depend on M , since the subhalo mass fraction in effect sets its normalization.

Following what was found by Weller et al. (2004); Shaw et al. (2005), we can then take the SHMF to have the form of a Schechter function:

$$N(m|M)dm = A_M \left(\frac{m}{\beta M}\right)^{-\alpha} \exp\left(-\frac{m}{\beta M}\right) \frac{dm}{\beta M}, \quad (3)$$

$$A_M = \frac{\gamma(M)}{\beta(\Gamma[2-\alpha] - \Gamma[2-\alpha, m_{\text{cut}}(M)/\beta M])}, \quad (4)$$

where α gives the low mass slope and β represents an additional cutoff mass. Typical values for the low mass slope α are around ~ 1.9 (De Lucia et al. 2004; Gao et al. 2004; van den Bosch, Tormen & Giocoli 2005;

Zentner et al. 2005), although Shaw et al. (2005) have found a less steep $\alpha = 1.75$ when fitting a power law and an even flatter $\alpha = 1.5$ when fitting to a Schechter function of the form of equation (3). We should also point out that van den Bosch, Tormen & Giocoli (2005) obtain a slope which varies slightly with parent halo mass. The cutoff value has alternatively been determined as $\beta = 0.13$ from semi-analytical models (van den Bosch, Tormen & Giocoli 2005), or $\beta = 0.3$ from simulations (Shaw et al. 2005). To this expression should be added the cutoff we are implicitly considering at m_{cut} , as expressed in equation (2). The first term on the right hand side guarantees that the mass fraction in subhaloes is $\gamma(M)$. From this we see that m_{cut} has essentially an effect on the normalization of the SHMF.

However, as discussed above, what we really require to build the non-parametric model is the original subhalo mass function instead. To do this, we apply the mass loss factor presented in the previous section to the SHMF of equation (3), that is, we use $m_{now} = f(m_{now}, M)m_0$, with $f(m_{now}, M)$ the mass loss function, renormalizing as appropriate to guarantee that the original total mass in subhaloes equals the present mass of the parent halo. In terms of the original mass m_0 , the SHMF of equation 3 then becomes

$$N_0(m_0|M)dm_0 = N[f(m, M)m_0|M]f(m, M) \times \left(1 - \frac{d\log f(m, M)}{d\log m}\right)dm_0, \quad (5)$$

where $f(m, M)$ is the mass loss factor, with m the present subhalo (i.e., the function plotted in figure 1); we have also explicitly included the transform of the differential term dm . Once more, we are implicitly assuming a cutoff at an original subhalo mass of $m = M/2$. Figure 2 shows different SHMFs calculated using this scheme.

There are some important conclusions to be drawn from figure 2. First, unlike the case with the present SHMFs, the original ones are almost universal when plotted as a function of m/M . This is a result of the fact that we are putting in what is, in these units, a universal normalization at the total halo mass M and also a universal cutoff at $m/M = 0.5$, which usually dominates over the one in equation (3), after transforming to the original mass. As a direct consequence of this, we can see that the original SHMF, as calculated through this method, is essentially independent of the present subhalo mass fraction γ and largely independent of the cutoff given by the parameter β . It is also largely insensitive to the shape of the mass loss factor as determined in the previous section. However, it should be cautioned that this depends on the actual mass loss factor f used: this is only true if it is fairly regular, or more precisely $d\log f/d\log m \ll 1$, as is mostly the case of the function we are using presently, which mostly causes a rescaling of the subhalo mass function, without much altering its shape. In such a case, in fact, the only parameter of the present SHMF which has a large effect is the low mass slope α . This indicates that it should be mostly correct, in the context of building a non-parametric model like we are doing here, to use as the original SHMF a power law of slope α , with a cutoff at $m/M = 0.5$ and the whole normalized so that the total original mass in subhaloes equals the present parent halo mass. From this, it is important to retain that,

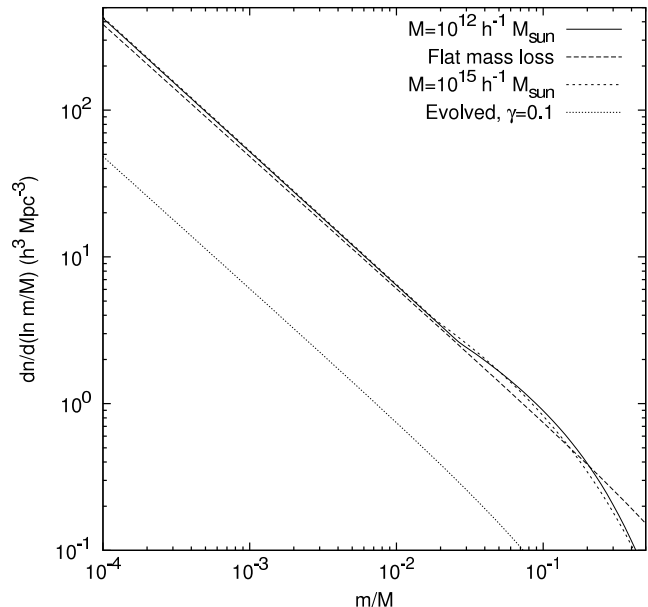


Figure 2. The subhalo mass function (SHMF): shown are the original SHMFs for parent haloes of mass $10^{12}h^{-1}M_{\odot}$ and $10^{15}h^{-1}M_{\odot}$. For comparison, we also show the original SHMF for a $10^{12}h^{-1}M_{\odot}$ halo when we take a flat mass loss factor, instead of one based on the curves of figure 1, and a present, evolved SHMF with a subhalo mass fraction of $\gamma = 0.1$.

accepting these two conventions we are using on the normalization and cutoff, the only element of the SHMF to which our model is sensitive is the low mass slope.

For the subsequent calculations, we will use a model with the mass loss factor calculated in the previous section, a present SHMF given by equation (3) with $\alpha = 1.9$ and $\beta = 0.3$. As mentioned above, the actual value of the mass fraction γ is not important since we have to renormalize the original mass function we obtain; it is only factored if we wish to have the appropriately normalized mass loss factor $f(m_{now}, M)$ to convert between original and present subhalo mass using $m_{now} = f(m_{now}, M)m_0$. Hereinafter, unless otherwise stated, all subhalo masses refer to the original mass.

4 BASIC MODEL

In this section we present our base model. We take a flat cosmology with parameters $\Omega_M = 0.25$, $\sigma_8 = 0.8$ and $h = 0.7$. While these do not exactly correspond to the current standard model (Bahcall et al. 1999; Spergel et al. 2003; Tegmark et al. 2004), they are within the allowed range of the $\Omega_m - \sigma_8$ plane determined from the joint WMAP-SDSS study of Tegmark et al. (2004), and we find they produce results better matching observations (see section 5.2 below) than do models with slightly higher (Ω_m, σ_8) . On the other hand, they match very well with the results found from an analysis of CMB and 2dF power spectrum by Sanchez et al. (2005), being near the center of their $\Omega_m - \sigma_8$ concordance region (see figure 3). For the basic model, we use the luminosity function in the K-band as determined from the Two Micron All-Sky Survey (2MASS; Jarrett et al. 2000). Using the K-band allows us to avoid possible complications and discrepancies arising from brief intervals of

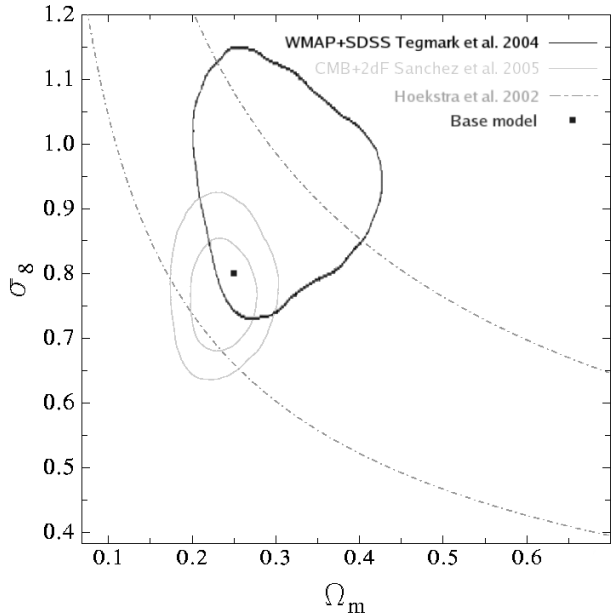


Figure 3. The $\Omega_m - \sigma_8$ plane. Shown are the 1- and 2 σ contours from the CMB+2dF power spectrum results of Sanchez et al. (2005), together with the 2 σ concordance region from the WMAP+SDSS results of Tegmark et al. (2004). Also shown as an example of weak lensing results are the constraints of Hoekstra, Yee, & Gladders (2002). The point marks the parameter values chosen for our basic model.

active star formation, and therefore helps present a clearer picture. We use here a single waveband for clarity in the construction of the model; a comparison of results for different wavebands using different luminosity functions is presented in section 5.1.

4.1 Host mass function

The first step to building the non-parametric model is to combine the above subhalo mass function with the parent halo distribution in the form of the halo mass function to obtain the global distribution of the dark matter hosts of galaxies. This is also the step where the cosmological parameter dependency is factored in, by determining the form of the mass function. We will use the Sheth-Tormen mass function (Sheth & Tormen 1999), given by:

$$n_h(M)dM = A \left(1 + \frac{1}{\nu^{2q}}\right) \sqrt{\frac{2}{\pi}} \frac{\rho_m}{M} \frac{d\nu}{dM} \exp\left(-\frac{\nu^2}{2}\right) dM, \quad (6)$$

with $\nu = \sqrt{a} \frac{\delta_c}{D(z)\sigma(M)}$, $a = 0.707$, $A \approx 0.322$ and $q = 0.3$; as usual, $\sigma(M)$ is the variance on the mass scale M , $D(z)$ is the growth factor, and δ_c is the linear threshold for spherical collapse, which in the case of a flat universe is $\delta_c = 1.686$. This mass function can be roughly approximated by a power law at low mass, scaling as $\sim M^{-1.95}$, and an exponential cutoff at high mass of the form $\exp(-M/M_*)$, where the cutoff mass is defined by $M/M_* \equiv \nu^2/2$ and we have roughly $M_* \approx 5 \times 10^{14} h^{-1} M_\odot$. The total distribution of dark matter hosts is then given by combining this with the global distribution of subhaloes, which can be calculated from the SHMF (3) and the halo mass function (6) by

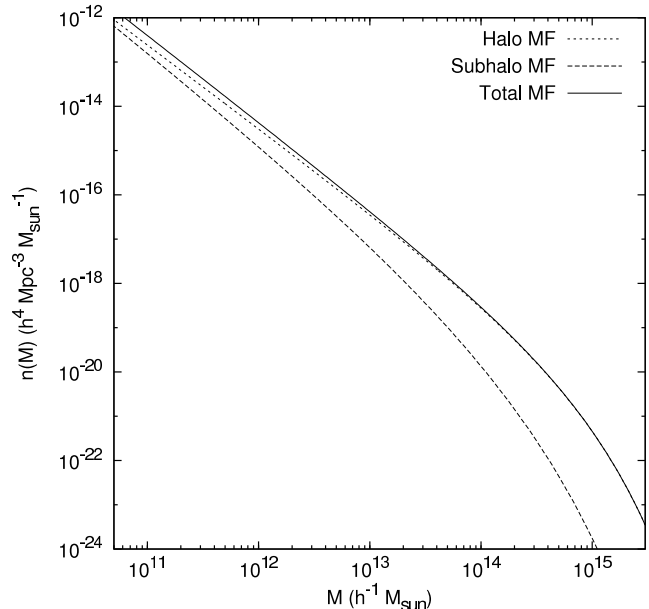


Figure 4. Global mass functions for haloes and subhaloes. In the case of the subhaloes, the x-axis refers to the original, unstripped mass (see discussion in text).

$$n_{sh} = \int_0^\infty n_h(M) N(m|M) dM. \quad (7)$$

These mass functions are shown in figure 4. Note that in the combined distribution of haloes/subhaloes the former dominate with subhaloes approaching parity only on mass scales below $10^{12} h^{-1} M_\odot$.

4.2 Luminosity Function

The galaxy distribution is accounted for by the galaxy luminosity function, which we assume takes the shape of a Schechter function (Schechter 1976):

$$\phi(L)dL = \phi_* \left(\frac{L}{L_*}\right)^\alpha \exp\left(-\frac{L}{L_*}\right) \frac{dL}{L_*}. \quad (8)$$

For this base model, we use the K-band results from the 2MASS survey, with parameters given by $\alpha = -1.09$, $\phi_* = 1.16 \times 10^{-2} h^3 \text{Mpc}^{-3}$ and $M_* - 5 \log h = -23.39$ (Kochanek et al. 2001) (see also table 1). In section 5.1 below, we analyse the result of using luminosity functions in other wavebands. This fit applies to the magnitude range $-22 > M_K - 5 \log_{10} h > -25$. An important point to note is that we will assume that the fit actually holds outside of this limited range, and extrapolate its result outside of it as necessary. This raises the question of how good a description of the real luminosity function a Schechter function is and, in particular, whether a power law is a good fit to the faint end. Observations at the faint end are plagued by a host of natural difficulties, most of all the need to sample efficiently low luminosity and low surface brightness galaxies. It is not yet entirely certain whether the luminosity function at the faint end can be well fit by the power law in the Schechter function over a wide range (see for example Trentham & Tully 2002; Trentham, Sampson & Banerji 2005; see also Blanton et al. 2005, who look at faint galaxies in SDSS and find that a Schechter function is a poor fit, and need to introduce a

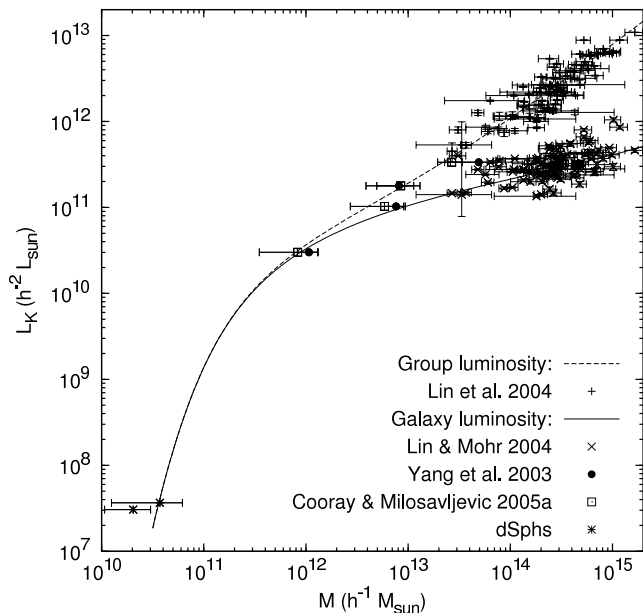


Figure 5. Mass K-band luminosity relation, both for single galaxies and total group luminosity (upper curve). Galaxy luminosity applies to both haloes and subhaloes, where the mass of the latter refers to the original, prior to accretion into the parent case. The data points shown come from Lin & Mohr (2004) and Lin, Mohr & Stanford (2004) (on cluster scales, for both total and brightest galaxy luminosity), analysis of SDSS weak lensing (Yang et al. 2003; Cooray & Milosavljević 2005a), and an estimate of Milky Way dwarf spheroidal mass and luminosity (see text for details).

double rather than single power law parametrization at the faint end). For now, we will simply assume that we can extend the measured faint-end slope of the 2MASS survey to fainter magnitudes than their stated limit.

4.3 Mass Luminosity relation

We can now combine the total dark matter host distribution with the galaxy distribution to get a relation between halo/subhalo mass and galaxy luminosity, by matching counts as described above in section 2. The resulting relation is shown in figure 5.

Also shown are observational data for brightest cluster galaxy luminosity and cluster luminosity versus cluster mass, taken from the K-band results of Lin & Mohr (2004) and Lin, Mohr & Stanford (2004). These studies use X-ray temperature results to determine the cluster mass together with luminosities taken from the 2MASS survey; we include a correction to the halo mass to account for a virial overdensity of 100 times the critical density (e.g., Bryan & Norman 1998), instead of 200, based on taking an NFW halo with a concentration of 5 as was done in Lin, Mohr & Stanford (2004) (see further discussion in section 5.3). The points at the low-end come from Milky Way dwarf spheroidal satellites, where the mass was estimated from results of Hayashi et al. (2003) (see also discussion in paper I) and the luminosity comes from the B-band results of Mateo (1998), then using an average $B - K = 3.6$ to convert to the K-band (Mobasher & Trentham 1998). The intermediate mass results come from an analysis of SDSS weak lensing results

in Yang et al. (2003) and Cooray & Milosavljević (2005b); in both of these, we have transformed the z-band luminosity to K-band by using $\log(L_K/L_z) = -0.014 + 0.492(g - r)$, with an average $(g - r) = 0.6$ (Bell et al. 2003). For all these cases, we again converted to M_{100} , using for the concentration the Bullock et al. (2001) model.

We find that the mass luminosity relation we obtain (figure 5) can be well approximated by a double power law of the type:

$$L = L_0 \frac{(m/m')^a}{(1 + (m/m')^{bk})^{1/k}} h^{-2} L_\odot, \quad (9)$$

with the parameters $L_0 = 1.23 \times 10^{10}$, $m' = 3.7 \times 10^9 h^{-1} M_\odot$, $a = 29.78$, $b = 29.5$, and $k = 0.0255$. This fit is good to within $\sim 6\%$ in the range $5 \times 10^{10} < M/(h^{-1} M_\odot) < 5 \times 10^{15}$. The most important fact to retain from this fit is that luminosity scales as $L \propto M^{0.28}$ at high mass. The high values obtained for the exponents a and b are an artifact of the fact that the relation is steepening as the mass decreases (note the value of the break mass given by m'). Group luminosity scales as $L_{\text{group}} \propto M^{0.88}$ for high halo mass. Overall, these parameters look different from the fit to observed data done using the same functional form as equation (9) by Cooray & Milosavljević (2005b). The main reason for the difference is the corrections we put in for the mass estimates. Also, as noted, care should be taken with the low mass slope, since the values for the best fit curve depend on the lowest mass used for the fit. It is, however, easy to predict this slope: if the mass function goes as $\sim M^{-a} dM$ (where this represents the total for haloes plus subhaloes) and the luminosity function as $\sim L^{-b} dL$, then the luminosity will scale as $L \propto M^c$, with $c = (a - 1)/(b - 1)$. With $a \simeq 1.95$ and $b = 1.09$, we get $c \simeq 10.5$.

Overall, these results seem a good match to the observations. The quality of this match has improved over the results we presented in paper I, especially for the group/cluster luminosity. As we had hinted in the discussion in paper I, this is most likely due to the fact that we now have a better, more self consistent, way of treating the subhalo mass fraction and mass loss. It is also interesting to note that, since we obtain a total luminosity which scales almost linearly with mass, we naturally obtain a mass to light ratio on cluster scales that is almost constant; this is intrinsic to the model, and is in good agreement with observations (see section 6.1 below). It is also worth to point out that the agreement for the group luminosity is not trivial: only the halo/subhalo mass-galaxy luminosity relation is constructed directly from the model. The group luminosity is obtained by assuming that applying this derived galaxy luminosity to the system of the haloes and their subhaloes will result in a good match for the corresponding galaxy systems. The agreement we obtain seems to point out that this is indeed a valid assumption (but see Cooray & Cen 2005 for some potential problems involving the detailed luminosity functions for individual groups when following this prescription).

There is some discrepancy between our results and the results for the higher mass bins based on weak lensing of SDSS galaxies (the points from Yang et al. 2003; Cooray & Milosavljević 2005a). While there is no straightforward way to explain the differences we find, we caution that there are several factors that, when taken together, may be enough to account for them. Most relevant of these are

the fact that we are using an average colour to change the luminosities from the z - to the K-band, and the possibility that the mass being accounted for does not correspond exactly to the definition we are using. Intriguingly, these weak lensing results seem to be a good match to our curve for the total luminosity, which raises the additional possibility that the observed luminosity includes not only the central lensing galaxy, but also some close, faint, satellites (since we would expect that most substructure in these medium mass parents to be relatively small).

5 DEPENDENCE ON LF AND COSMOLOGY

5.1 Luminosity function

In this section, we look at how our base result for the mass luminosity relation changes depending on the luminosity function (and consequently waveband) we use as a starting point. We use a variety of published luminosity functions, listed in table 1, ranging from the blue to the infrared, and repeat the analysis of the previous section for each of these. The results for the galaxy and total luminosity are shown in figure 6, where the luminosity is plotted in units of the characteristic luminosity L_* of each of the luminosity functions.

The most striking feature of these results is that galaxy luminosity in high mass haloes is almost independent of the luminosity function used, with only very slight differences due to different normalization and faint end slope. Technically, this is a consequence of the fact that all luminosity functions considered have a bright end cutoff of the form $\exp(-L/L_*)$. In general, galaxies have an observed colour-magnitude relation which should be reflected in a different mass-luminosity relation at different wavebands (as is the case here for lower mass). In this particular case, however, almost all the galaxies for these high mass haloes will be brightest cluster galaxies, for which an almost flat colour-luminosity relation is expected (see e.g. Eisenstein et al. 2001), in agreement with the model results. The scaling at this high-mass end goes as $L \propto M^{0.28}$. This is similar to that obtained in other studies using the conditional luminosity function formalism, like Cooray & Milosavljević (2005a), who find that the central galaxy luminosity scales as $\sim M^{0.3}$ for high halo mass, while the total luminosity of the galaxies in the halo scales as $\sim M^{0.85}$ in the K-band; using 2dF results, Yang et al. (2005) also find that the luminosity of the central galaxy scales as $L_c \sim M^{0.25}$. A fit to the observational K-band data gives $L \propto M^{0.26}$ (Lin & Mohr 2004).

For low mass haloes and subhaloes, there are large differences between the results obtained by using the different luminosity functions. These are mostly a product of the characteristic luminosity, which determines where the break in the mass luminosity relation occurs, and the faint end slope, which determines the slope in the relation for low mass. These results illustrate the importance of an accurate determination of the faint end slope to obtaining a good mass luminosity relation. Nonetheless, looking at the results for the group luminosity it is possible to see that these differences have only a small effect when calculating the total luminosity associated with a high mass halo. The different results are quite close, particularly in terms of scaling, if

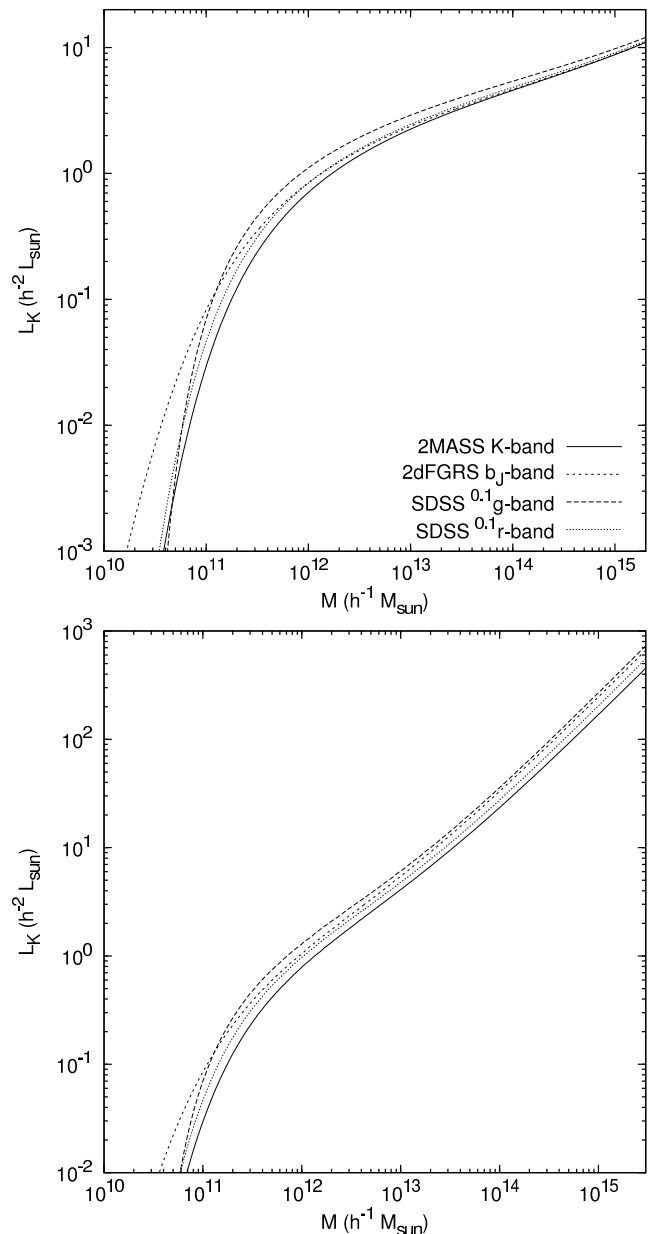


Figure 6. Comparison of the galaxy (upper panel) and group (lower panel) luminosities obtained when using the non-parametric model described in section 4 with the different luminosity functions of table 1. The luminosities have been scaled by the characteristic luminosity L_* of the luminosity function used.

less so than in the individual galaxy case, and the differences seem mostly due to the characteristic luminosity L_* . There is in fact some observational evidence that the scaling of cluster luminosity with mass is independent of photometric band (see e.g., Popesso et al. 2004). Since the brightest galaxy luminosity gives a small relative contribution for high mass systems (cf figure 5), it is possible to conclude that the main contribution to the luminosity should come from relatively massive subhaloes with luminosities roughly above $0.1L_*$, below which the differences due to the low end slope become quite significant, mostly due to different faint end slopes in the luminosity functions. More importantly, this means that the mass-total luminosity relation obtained by

Band	$\phi_*(10^{-2}h^3\text{Mpc}^{-3})$	α	$M_* - 5\log h$	Ref.
K	1.16 ± 0.10	-1.09 ± 0.06	-23.39 ± 0.05	2MASS (Kochanek et al. 2001)
b_J	1.61 ± 0.08	-1.21 ± 0.03	-19.66 ± 0.07	2dFGRS (Norberg et al. 2002)
$^{0.1}g$	2.18 ± 0.08	-0.89 ± 0.03	-19.39 ± 0.02	SDSS (Blanton et al. 2003)
$^{0.1}r$	1.49 ± 0.04	-1.05 ± 0.01	-20.44 ± 0.01	SDSS (Blanton et al. 2003)

Table 1. Schechter function parameters of the luminosity functions used.

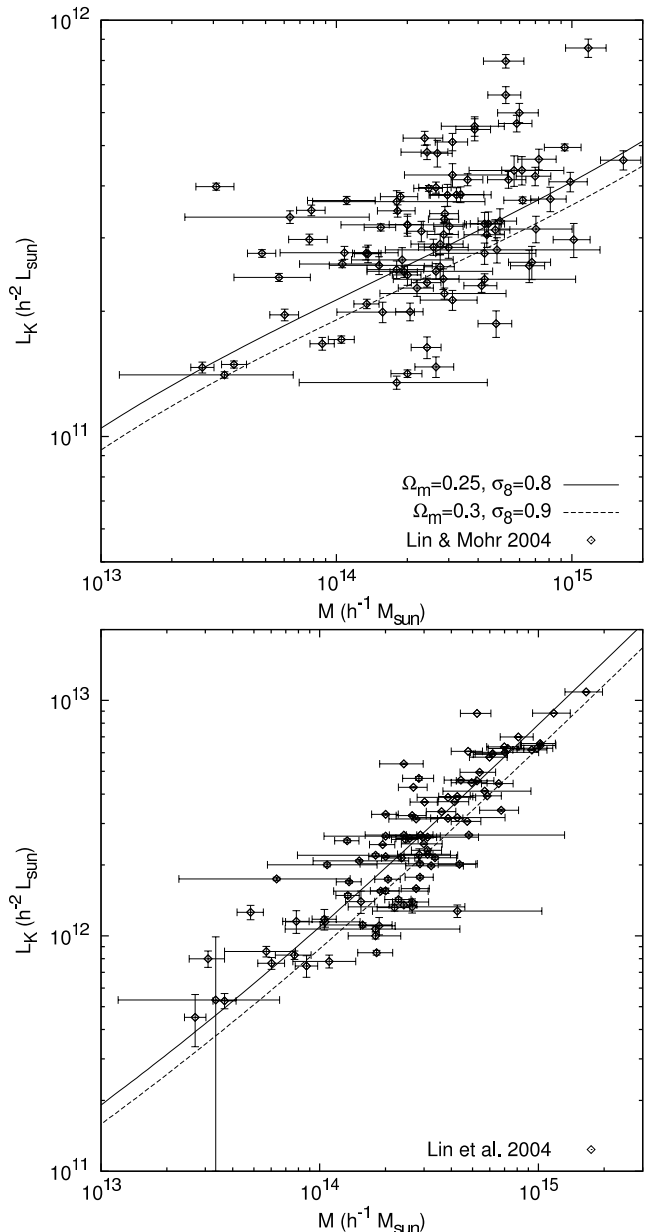
the non-parametric model depends mostly on the more well determined of the luminosity function parameters, L_* .

5.2 Cosmological parameters

Although the agreement between our results and the large observational data set of brightest cluster galaxy luminosities and halo masses shown in figure 5 was fairly good, it is possible to see that our model tends to slightly underpredict the expected luminosities. At such high masses, the subhalo contribution to the total host number and therefore to the mass-luminosity relation is negligible (see figure 4), and, as we have shown in the previous section, the results are also largely independent of the luminosity function. Therefore, the relation between halo mass and hosted brightest galaxy luminosity depends essentially on the halo mass function, and through it on the cosmology considered. This makes it important to look at the background cosmology used and how it affects the results.

An example of this is shown in figure 7, where we also show the observational data for comparison. In general, it is possible to conclude that, comparing with the observations, our model tends to prefer lower values of Ω_m and σ_8 . The technical reason for this is quite straightforward: lower values result in fewer high mass haloes, which means that when comparing to observed galaxy numbers it results in higher luminosity galaxies being associated with the same halo mass. For this reason, we have adopted in our calculations a cosmological model with $\Omega_m = 0.25$ and $\sigma_8 = 0.8$, rather than the more standard $\Omega_m = 0.3$ and $\sigma_8 = 0.9$. This combination of values lies roughly on the lower edge of the concordance region from WMAP+SDSS measurements of Tegmark et al. (2004), and near the center of that from CMB+2dF (Sanchez et al. 2005) (see figure 3).

In fact, it is possible to obtain an even better agreement with the plotted observational values if we lower σ_8 further. There are two main reasons for not adopting such a model: first, the Tegmark et al. (2004) results represent the best current measured estimate for the combination of the two; second, and more importantly, there are further additional sources of error which are probably more significant than what is now a very accurate determination of the cosmological parameters. The first of these is the possibility that the main assumptions of the model are wrong. Mainly, that is that we cannot treat the mass luminosity relation as one-to-one and monotonic. While this is certainly true in specific cases and we expect there to be significant scatter about the relation, it seems a fair assumption to make for the average relation as we are determining here; going beyond this assumption is outside the scope of this model. Second, and more importantly in the context of the present paper, there is the possibility that the model is giving incorrect results simply because the number functions we are

**Figure 7.** Derived mass-luminosity relation for galaxies (upper panel) and groups (lower panel) as a function of the cosmological model used, for $\Omega_m = 0.25$, $\sigma_8 = 0.8$ and $\Omega_m = 0.3$, $\sigma_8 = 0.9$.

using as a basis for the comparison are mismatched, that is $n(m)_{\text{observed}} \neq n(m)_{\text{model}}$, where the observational term applies to the data points we are comparing our results with. Since the method is based on counting numbers for each of these, a difference between them would cause it to give incorrect results when comparing to observations. As we discussed above, the cosmological model used can change the

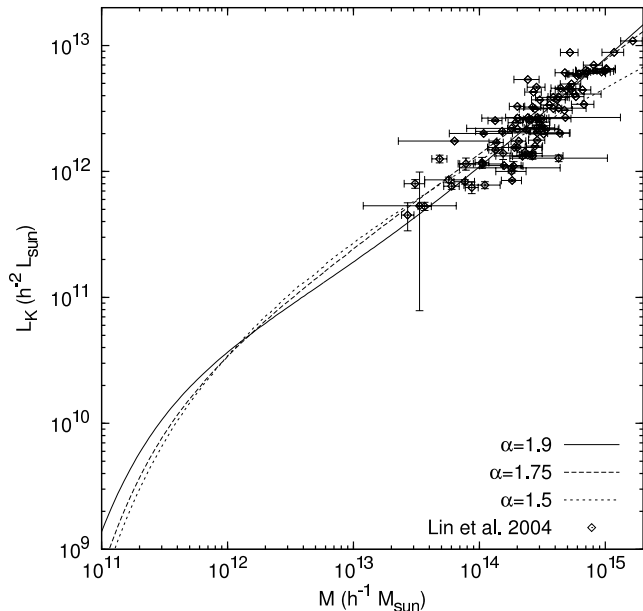


Figure 8. Group luminosity obtained by varying the low mass slope of the subhalo mass function, equation 3, between $\alpha = 1.5$ and $\alpha = 1.9$ (our base model).

model part of the equation. Far more likely, though, is that we are using an incorrect estimate for the observed mass that is skewing the observed term. We discuss this issue further in the next section.

It is also worthwhile noting that, once the cosmology is fixed, the main determinant for the form of the halo mass-total luminosity relation is the slope of the subhalo mass function. This assumes that its normalization and cutoff are predefined, as discussed in section 3.2. Figure 8 shows the result of varying this slope. Generally, a flatter slope for the subhalo mass function results in a flatter slope at high halo mass for the total luminosity as well. Since a fit to the observational data gives a slope of 0.72, while we obtain 0.88, using a flatter slope for the subhalo mass function than 1.9 (quite possible in light of simulation results; see Shaw et al. 2005) would likely give a better agreement with observations, depending on possible corrections to their mass estimates, which may not be uniform. It should be noted, however, that this in fact applies to the original subhalo mass function slope. How it compares with the present slope depends on the mass loss factor. With the one we are using in this paper, the slopes are mostly equal (see section 3).

5.3 Observed mass determination

As noted, one of the possibilities that may explain the difference between our model results and the set of observational cluster data as presented in figure 5 is a potential misestimation of the corresponding halo mass. First of all, there is the problem of how to extrapolate to the virial mass. In Lin, Mohr & Stanford (2004), the authors determine M_{500} , the mass enclosed in a radius where the average density is 500 the critical, from X-ray temperature measurements. Besides the actual observational error in the temperature, and possible errors in the $M_{500} - T_X$ relation used (which are assumed to be accounted for in the observational error bars),

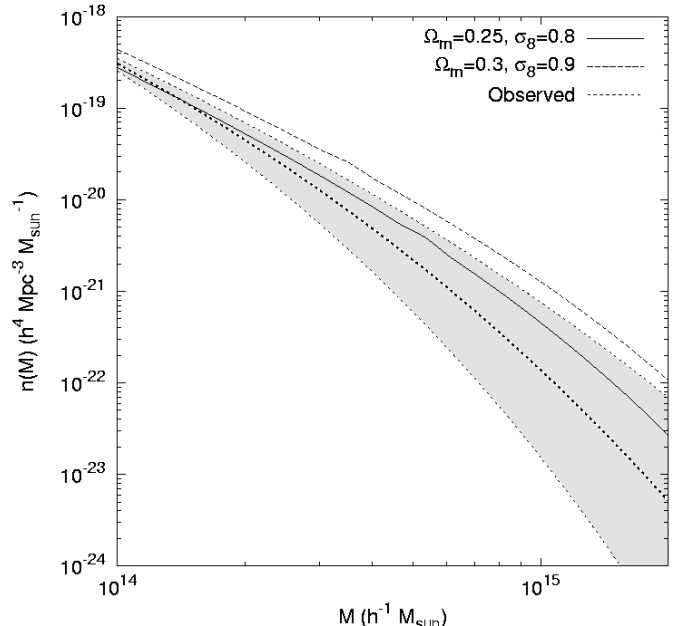


Figure 9. Halo mass function for our base model, together with the corresponding mass function for clusters as derived from the observed luminosity function and cluster halo mass-central galaxy luminosity relation (see text for details); the central line comes from the fit found by Lin & Mohr (2004), the lines above and below represent the 1σ range from the fit. Also shown is the curve for the $\Omega_m = 0.3$, $\sigma_8 = 0.9$ halo mass function, for comparison.

there is the problem of how to extrapolate M_{500} to the halo virial mass. Following what is done by Lin, Mohr & Stanford (2004), we assume an NFW halo with a concentration of 5 to calculate the virial mass, except that we take the virial radius to be at r_{100} rather than r_{200} . A different density profile or simply concentration would result in a different measure for mass. Changing the concentration to a value in the range of between 4 and 7, for example, could result in as much as a 10% shift upwards or downwards in the estimated mass.

The non-parametric model cannot work if the halo mass function for the assumed cosmology does not match observations, but there is a relatively straightforward way of checking how well these mass estimates agree with the results from our model. As mentioned previously, that is to check whether the predicted galaxy number at a given halo mass from the observed values match the number in the model, $n(m)_{\text{observed}} = n(m)_{\text{model}}$, where $n_{\text{model}}(m)$ in the high mass range we are interested in here is given by the halo mass function. As noted, these two must match if the comparison between the model and the data is to be meaningful, since the model is based on counting numbers. In order to determine $n(m)_{\text{observed}}$, we combine the luminosity function with the fit to the observed halo mass-brightest cluster galaxy luminosity relation from Lin & Mohr (2004). The resulting mass function, together with the possible range obtained from the errors in the fit parameters, is shown in figure 9. From this we can see that, while the halo mass function we are using does not quite match the mass function corresponding to the observations, it is well within the range allowed by the fit errors. If we assume that the results from the

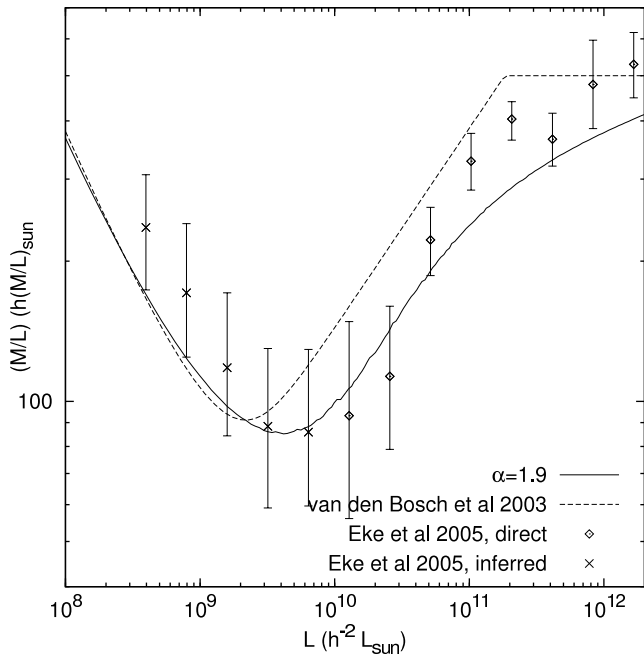


Figure 10. Mass to b_J -band light ratio of galaxy systems (from isolated galaxies, to groups and clusters with growing mass). Data points are taken from the corrected mass to light ratio calculated for the 2PIGG catalogue of the 2dF survey by Eke et al. (2005). These include both the directly measured values for luminosities above $L > 10^{10} h^{-2} L_{\odot}$, and the values inferred by comparing the derived group luminosity function with a theoretical mass function, for luminosities below this threshold. The latter were extracted from the shaded region in figure 15 of Eke et al. (2005), where the point represents the value of their model curve at that luminosity. The errorbars include uncertainties related to different possible values of σ_8 . For comparison, we also show a line for the result of model D of van den Bosch, Yang & Mo (2003).

model are essentially correct, we can then use these curves to calculate a further correction to the estimated mass. In fact, this corresponds to finding the transformation that matches the fit to the observed data to our result for the average mass-luminosity relation.

6 ADDITIONAL CHECKS

In this section we calculate an additional four results which can be derived directly from our non-parametric model, and which can be used as an additional check on the success of the model: the mass to light ratio, the occupation number, the group luminosity function and the multiplicity function.

6.1 Mass to light ratio

The discussed trends of the mass-luminosity relation are further visible in figure 10, which shows the b_J -band mass to light ratio of the entire system (that is, a group or cluster if massive enough; this is basically a different way of plotting the result of figure 5).

As mentioned above, at the high mass end the cluster luminosity is almost directly proportional to halo mass (roughly, $L \propto M^{0.88}$). This means that the resulting mass to light ratio will be almost constant, as can be seen in

the figure, rising only very slowly with halo mass, which matches well with previous results for the mass to light ratio of clusters (e.g., Bahcall et al. 2000; Kochanek et al. 2003; Eke et al. 2004, 2005). In this case, though, the values we obtain for the mass to light ratio seem to be slightly smaller than the observational results at the bright end, otherwise they seem in good agreement. This is reflected in the values for the cluster mass to light ratio. The value derived by Fukugita, Hogan & Peebles (1998) is $450 \pm 100 h(M/L)_{\odot}$, while Eke et al. (2004) obtain an average value of $466 \pm 26 h(M/L)_{\odot}$; we obtain a slightly lower cluster mass to light ratio of approximately $425 h(M/L)_{\odot}$ for a $10^{15} h^{-1} M_{\odot}$ halo. Since we obtained a good agreement with the cluster luminosity results of Lin, Mohr & Stanford (2004) and, as discussed above, the mass luminosity for single galaxies is well constrained in our model, the most likely origin for the discrepancy we find here is likely to be the subhalo distribution. Lowering the value of the subhalo mass function slope slightly results in a better agreement with the observational results at both the low and high luminosity ends; however, the agreement is poorer at intermediate luminosities, while the slope of the derived mass to light ratio becomes steeper (cf. results in figure 8).

We can also compare our results with the conditional luminosity function of Yang, Mo & van den Bosch (2003). Plotted in figure 10 is the result of the average halo mass to light ratio fit with the parameters of model D of van den Bosch, Yang & Mo (2003). There is a good agreement at the low end, while again we find some disagreement at the high end. Note that this disagreement is most likely due to the fact that we are adopting a different cosmology than these authors, with slightly lower values for Ω_m and σ_8 . Nevertheless, the overall shape is quite similar; the small difference is most likely due to the factor that these authors are fitting the mass to light ratio to a double power law, with a sharp transition to a constant at high mass, while we obtain a smooth function. The minimum also occurs at a slightly higher luminosity. We are actually in better agreement with the observed values at an intermediate range (around $10^{10} - 10^{11} h^{-2} L_{\odot}$), while the opposite happens at the bright end. Between both results is considerably better; as noted, using a flatter slope for the subhalo mass function may help with the problem.

Figure 10 also illustrates quite well the various mass (or, as presented in the figure, luminosity) scales which determine galaxy properties (cf. Dekel 2004). There is a minimum in the mass to light ratio at a mass scale of around $3 - 4 \times 10^{11} h^{-1} M_{\odot}$. This is a good match for the scale which represents a shift in the characteristic galaxy population corresponding to a change in the sources of gas accretion and star formation suppression (e.g., Dekel & Birnboim 2004). Also, as we have already shown, the steep slope in the mass luminosity relation means that haloes below roughly a few times $10^9 h^{-1} M_{\odot}$ will essentially be dark; again, this matches well with the mass below which photoionization is expected to suppress gas infall (Babul & Rees 1992; Thoul & Weinberg 1996; Dekel & Woo 2003). At the high end, there is a noticeable break in the mass to light ratio at a corresponding mass of around $10^{13} h^{-1} M_{\odot}$. As can be seen in figure 5, this marks the scale where we go over from isolated galaxies with at most very small satellites to actual groups, and once more is in good agreement with

what is observed and expected from a theoretical point of view, which predicts an upper bound for cooling in a dynamical time at this mass scale. This is also the mass scale at which merging is expected to become inefficient (e.g., Cooray & Milosavljević 2005a).

6.2 Occupation number

With the subhalo mass function given by equation (3), it is straightforward to calculate the occupation number (that is, the number of subhaloes in a parent halo of given mass), as a function of halo mass M . This is simply given by:

$$N_s(M) = \int_{m_{min}}^{\infty} N(m|M) dm. \quad (10)$$

The only complication is that it is necessary to specify a minimum mass for the subhaloes, m_{min} ; otherwise, the integral is divergent. Since we equate subhaloes with satellite galaxies, we can associate this minimum mass with a minimum luminosity of these galaxies, and then $N_s(M) + 1$ will give us the total number of galaxies in a halo of mass M , with luminosity greater than the minimum we are considering; this is one of the key ingredients of the HOD models, (e.g. Berlind & Weinberg 2002; Zheng et al. 2004; Yang et al. 2005). These models usually take the function in (10) to be the average value of the number of satellite galaxies, with the actual number a Poisson distribution around this average; this seems to be in good agreement with simulation results (Kravtsov et al. 2004; Zheng et al. 2004). Also, the occupation number of the central galaxy is usually taken to be a step function, being 0 or 1 depending on whether the halo mass is greater than a certain minimum; the case in our model is also similar, as we consider that a halo hosts a galaxy with luminosity above a certain threshold if its mass is greater than that corresponding to this luminosity from the mass-luminosity relation. Our results for the occupation number are shown in figure 11, where we take the minimum mass to be the necessary to host a galaxy with $M_K = -21$. The points plotted are taken from the cluster data of Lin, Mohr & Stanford (2004), where as before we have included a correction to the mass.

Our result is in quite good agreement with the plotted data. At high halo mass (approximately above $\sim 10^{13} h^{-1} M_{\odot}$), our result for the occupation number scales roughly as $N \propto M^{0.9}$. Qualitatively, it also compares well with those obtained from simulations, analytical models and observations by a variety of authors. The first thing to note is that, unlike the result in paper I, the occupation number is now no longer a function of M/m_{min} alone: there is an extra dependence on the halo mass M . Physically, this is understandable as haloes having $M/M_* > 1$ are in the process of growing and merging whereas those having $M/M_* < 1$ are decreasing in number density as they merge into larger systems. This is a consequence of the fact that the subhalo mass function, given in equation (3), cannot be written as a function of solely m/M : its normalization has terms which depend only on M . While a direct comparison of the numbers is complicated by the fact that they depend on what mass threshold is being considered, the slope of the occupation number for high mass haloes is roughly the same as that found in other studies. This matches well with

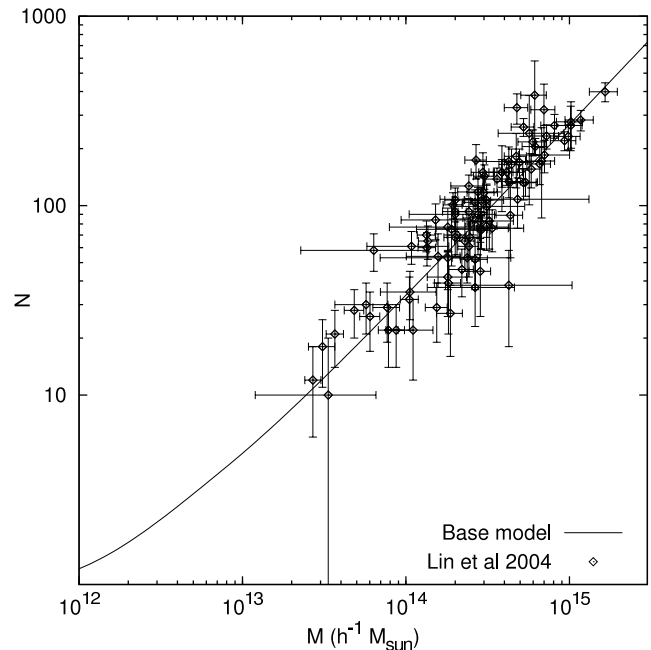


Figure 11. Occupation number: average number of galaxies predicted for a parent halo of mass M , given by the sum of the number of subhaloes with galaxies above a given luminosity plus one for the central galaxy. The luminosity threshold adopted was $M_K < -21$, which corresponds to the minimum used for the observed data points plotted, taken from Lin, Mohr & Stanford (2004).

the analytically derived halo mass function of Oguri & Lee (2004), who find a slope of 0.9 at high $M/m \approx 10^5$, and closer to 1 at lower $M/m \approx 10^2$, and also with the results from simulations: for example, Kravtsov et al. (2004) find a slope very close to 1, while Zheng et al. (2004), in fitting HOD models to semi-analytic models of galaxy formation and smoothed particle hydrodynamic simulations, find values for the slope between 0.97 and 1.24 (depending on the baryonic mass threshold). Results of observational studies also seem to agree on a slope of about 1: Kochanek et al. (2003) obtain a relation for the number of galaxies with $L > L_*$ scaling as $M_H^{1.1}$, while Abazajian et al. (2005) fit a HOD model, together with the cosmological parameters, to the projected correlation function of a volume limited subsample of the Sloan Digital Sky Survey (SDSS), together with CMB results, and find a good agreement with models where the slope is fixed at a value of 1; when they leave this as a free parameter, they obtain a result of 0.8, but without a significant improvement in the quality of the fit.

6.3 Group luminosity function

Also of interest when studying clusters is the group luminosity function, $\phi_g(L_g)$. This is the analogous of the galaxy luminosity function, but is calculated for groups and clusters, and gives the number density of these objects in a given luminosity range. We can obtain this in our model by transforming the mass dependent halo mass function by using the relation between halo mass and total group luminosity:

$$\phi_g(L_g) dL_g = n_h(M(L_g)) \frac{dM}{dL_g} dL_g. \quad (11)$$

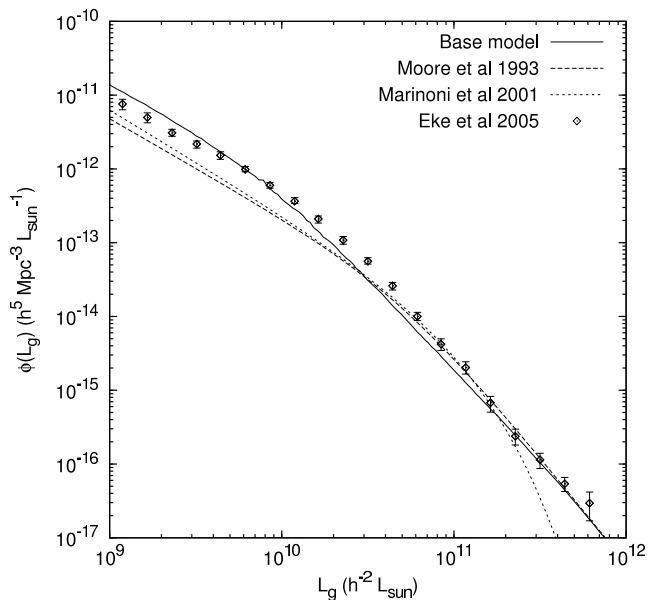


Figure 12. Group luminosity function. The solid red line represents the result of the non-parametric model using equation (11); the two other lines are observational group luminosity functions extracted from galaxy catalogues, respectively the AGS (Moore, Frenk & White 1993) (dotted) and the VSLF (Marinoni, Hudson & Giuricin 2002) (dashed).

Here, we are implicitly assuming that a group/cluster is made up of two components: a central galaxy hosted in the parent halo itself, and its satellites, hosted by the subhaloes. Thus the total luminosity is the sum of these two contributions:

$$L_g(M) = L(M) + \int_0^\infty L(m)N(m|M)dm. \quad (12)$$

This group luminosity is the same as was presented in figure 5 above. Our result for the group luminosity function is shown in figure 12. The determination of the observational function is usually done from galaxy catalogues by building groups of gravitationally bound galaxies. In the figure, we show the luminosity function fits of two different such functions: the AGS for the CfA survey (Moore, Frenk & White 1993) and the VSLF (Marinoni, Hudson & Giuricin 2002) group luminosity functions. We also show data for the group luminosity function as measured from 2dF results of Eke et al. (2005). We have included corrections to the AGS results by using $b_J = B_{\text{Zwicky}} - 0.05$ and making the VSLF results 0.55 magnitudes fainter to compensate for the difference between the B and b_J bands and internal absorption (see comments in Eke et al. 2005). We obtain a very good agreement with the observational results. This agreement is markedly better than the result in paper I; this is essentially a result of the higher group luminosity we obtain for each halo, which in turn is caused by an increase in the subhalo numbers at a given luminosity due to the more self-consistent way in which we are treating mass loss.

6.4 Multiplicity function

It is also possible to derive the multiplicity function, the number density of group/clusters as a function of their rich-

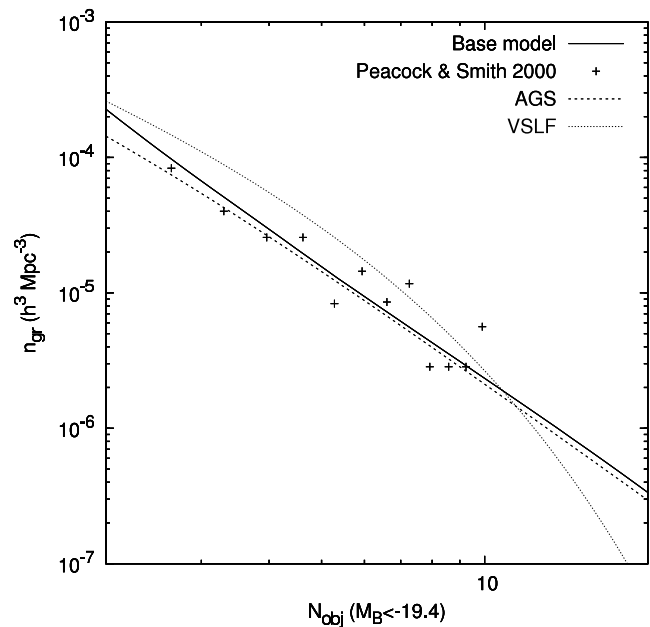


Figure 13. Multiplicity function derived from the non-parametric model (solid line), based on combining the halo mass function with the total halo occupation number, that is, the total number of galaxies, above a given luminosity, present in a parent halo. The minimum mass for the halo or any of its subhaloes to be counted corresponds to a magnitude of $M_B = -19.4$. The different points are taken from the results derived by Peacock & Smith (2000) from the CfA survey, while the two additional lines are estimates based on the group luminosity functions shown in figure 12, where the magnitude limit for all of these is also $M_B = -19.4$.

ness, by a process similar to the one described above for the group luminosity function. To do this, we replace the group luminosity L_g in equation (11) with the number of galaxies present in the halo. This is given by the total occupation number calculated above and shown in figure 11, that is, the number of luminous subhaloes plus one. The only other thing that is necessary to take into account is the limit to the galaxy luminosity we want to consider. This will then give a lower limit to the mass of the haloes and their subhaloes to put into the occupation number calculation. Our results for the multiplicity function are shown in figure 13. We have taken as the lower luminosity limit $M_B = -19.4$, in order to match the observational results also shown. Due to the way in which it is built, there is a sharp upturn at $N = 1$ due to the haloes which are massive enough to contain a galaxy but not to have subhaloes big enough to host a galaxy themselves. This is in part a consequence of modelling the occupation number of the parent halo as a step function, as was done above; a more realistic model would have a smoother transition (see e.g. Zheng et al. 2004 for an example of how this is done in the context of HOD models), which would help to attenuate this.

Figure 13 also shows some observational data. The points were taken from the analysis of Peacock & Smith (2000), while the two lines were constructed from the two group luminosity functions shown in figure 12. To do this, we assume that the luminosity function of the galaxies in each group has the same shape as the general galaxy luminosity function of the survey, a Schechter function with

characteristic luminosity L_* and faint end slope α , but with the normalization n determined by the group luminosity. By integrating this function, the group luminosity L_g can then be calculated as $L_g = nL_*\Gamma(2-\alpha)$; this is then related to the number of galaxies in the group above a certain threshold luminosity L_{min} by

$$N = \frac{L_g}{L_*} \frac{\Gamma(1-\alpha, L_{min}/L_*)}{\Gamma(2-\alpha)}, \quad (13)$$

where we used the expression above to replace n . Finally we can use this relation between group luminosity and member numbers in the group luminosity function to obtain the multiplicity function, using $n(N) = \phi_g(L_g)dL_g/dN$, where $n(N)$ and $\phi_g(L_g)$ are the multiplicity and group luminosity functions, respectively. The galaxy numbers for both the points and the results derived from the group luminosity functions were then multiplied by a factor of 0.66 to take into account the difference in radius between friends of friends estimates and the usual definition of virial radius (see Kochanek et al. 2003).

We obtain a good agreement with the observational points, better than was the case in paper I. This is not surprising given the results we presented above for the group luminosity function, and the root cause is the same: the more self-consistent treatment of mass loss has resulted in an increase in subhalo numbers at a given mass. On the other hand, at high member count, our result would seem to be above the multiplicity functions calculated from the group luminosity function. This is most likely due to the fact that we assumed above that we can use for the luminosity function of the group galaxies the same shape as the background luminosity function; while this should be true for moderately dense regions (corresponding to low N), it is not a very good approximation for very dense environments like clusters, where N is high (see Croton et al. 2005 for observational results). In fact, a higher L_* , expected in clusters with high N , gives a higher value for the multiplicity function, therefore bringing the two curves into better agreement with our results.

7 CONCLUSION

In this paper we have presented a non-parametric model to relate the luminosity of a galaxy to the mass of the halo or subhalo hosting it. We start by assuming that this relation is one to one and monotonic, and then compare their number as given by their statistical distributions, obtained from observations and simulations, respectively. This gives us the average relation between the luminosity of a galaxy and the mass of the dark matter halo or subhalo which hosts it. We can also determine the total group luminosity as a function of halo mass by integrating over the luminosity of all the subhaloes in a given parent.

We have argued that, to maintain the assumption of monotonicity, when accounting for the subhaloes it is in fact necessary to consider not their present mass, but rather their original mass just prior to accretion into their parent halo. In order to allow for this, we have introduced a simplified prescription for the average mass loss factor that we can then apply to subhalo mass functions measured from simulations to regain the original subhalo mass function. We

have noted that, however, there are two strong constraints on this function: first, no subhalo could originally have more than half the present mass of the parent halo, otherwise it would be, by definition, the parent halo itself; second, it is to be expected that, since the parent is built up by accreting and stripping mass off the subhaloes, that the total mass in the original subhaloes equals the present mass of the parent halo. If the mass loss factor is fairly regular (or more precisely, its logarithmic derivative is always significantly lower than 1, which is mostly the case with the one we presented), and assuming a present day Schechter type subhalo mass function (which seems to be obtained from simulation results; see e.g., Shaw et al. 2005), these two constraints mean that the only free parameter in the original subhalo mass function would be the low mass slope, which in these circumstances would be close to the present day one.

We find that, for high mass haloes, the mass-luminosity relation appears to be mostly independent of the luminosity function being used, when the luminosity is scaled to the characteristic luminosity L_* . The same is true, to a rather lesser extent, of the mass-group luminosity relation, which has an increased dependence on L_* . At the low mass end, the break in the relation is associated with L_* , while the slope depends significantly on the faint end slope of the luminosity function.

Overall, our results are a good match to observations and results of other theoretical models. We find, however, that for high mass haloes, our results seem to slightly underestimate the luminosity of both central galaxies and clusters when compared to the observational results of Lin, Mohr & Stanford (2004) and Lin & Mohr (2004). This small discrepancy between our results and observational data simultaneously raises some concern. The reason is that, as we have discussed, the mass luminosity relation in high mass haloes is practically independent of both the actual luminosity function used and of the subhalo population. This means that our result depends only on the halo mass function, and through it, on the cosmological model. We have shown that, when comparing our results with observations, our model seems to prefer lower values of Ω_m and σ_8 ; within the concordance region of Tegmark et al. (2004), best results are obtained near the lower boundary, and consequently we have used $\Omega_m = 0.25$ and $\sigma_8 = 0.8$ to construct our base model. While to change our result would necessitate changing the cosmology, or more seriously, the central assumptions underlying the model, it is far more likely that the discrepancy is actually a product of a misestimation of the observed halo mass. In fact, there is some uncertainty regarding the values of the mass cited in these studies, specifically in extrapolating them to the virial radius. A reasonable change in the concentration used to make this extrapolation may account for as much as a 10% shift in the estimated observed mass. Further, using the fit to the observed mass-luminosity data and the luminosity function, we have compared the expected number of galaxies in haloes of a given mass to the one we are using. We find that, while the agreement is not perfect, the mass function we used is well within the error range of the observed one. Further, assuming that our model is correct, it is possible to view the required transformation to the estimated mass to match the two curves as an additional correction to it.

The situation with the total luminosity on cluster scales

is relatively similar, though here the problem might be more one of shape rather than normalization. The slight discrepancy between our results and the observational data may be improved if the halo mass has been underestimated observationally or by tweaking with the cosmological parameters. There is however an additional factor, in that the subhalo population contributes significantly to the total luminosity. This is represented by the original subhalo mass function, and we have argued that its normalization and cutoff mass should be considered fixed, the former to give the total present parent halo mass, the latter to avoid having subhaloes which originally had more than half the parent mass. If we assume that this function has a Schechter shape (as would be the case with a present subhalo mass function with a Schechter shape and a regular mass loss factor), then the only free parameter left is the low mass slope. We have also argued, by comparing the results obtained using different luminosity functions, that the more important luminosity function parameter that determines the result at this high mass end is the characteristic luminosity L_* , while the faint end slope (which could be considered the most uncertain of the parameters) does not seem to be as big a factor. Therefore, if we take the subhalo mass-galaxy luminosity relation (and consequently the cosmology) to be fixed, the remaining free parameter in the model is the subhalo mass function low mass end slope.

On the one hand, this means that we cannot much vary the total number of satellite galaxies in this framework. On the other hand, our result for the group luminosity seems to be a better match to the observed values than that of the galaxy luminosity; if we were to increase the latter, we might end up obtaining too high a luminosity in groups, assuming the slope of the subhalo mass function is kept fixed. This potential problem may however be viewed in light of the recent results of Cooray & Cen (2005), who claim that when using a similar prescription to model the satellite galaxy luminosity function using the subhalo mass function, it is necessary to introduce an efficiency function lowering the number of luminous subhaloes otherwise predicted to match the two. There is also the possibility, which we have not considered, that the mass-luminosity relation is different for haloes and subhaloes; using a different relation for the latter might explain the difference to the observational results. Since gas accretion and mergers stop in subhaloes once they are accreted, we are led to the conclusion that, if this were to be the case, the subhaloes would actually be less luminous than what we are considering. Additionally, there is the effect of the slope of the subhalo mass function. Using a flatter slope than the 1.9 value we have used for our base model may help with this situation, since it would flatten the slope of the group luminosity calculated without changing the high mass galaxy luminosity. This may be beneficial, since the fit to the observed clusters from Lin, Mohr & Stanford (2004) goes as $L \propto M^{0.72}$, while we get a slightly steeper 0.88. If we do accept the whole framework of the model, though, this raises an intriguing possibility: the only free parameter we have is the low mass end slope of the subhalo mass function, and so we may be able to get a completely independent confirmation of its value by fitting the model results to the observational data.

Quantitatively, we find that central galaxy luminosity scales with halo mass as $L_1 \sim M^{0.28}$ for high mass haloes,

fairly independently of waveband when the luminosity is scaled by the appropriate characteristic luminosity L_* , and also of the form of the subhalo mass function. The total group luminosity scales with halo mass as $L_{tot} \sim M^{0.88}$, also fairly independently of waveband when appropriately scaled; a flatter subhalo mass function low mass slope results in a flatter dependence at the high mass end. This implies that the halo mass-to-light ratio is almost flat at high mass (and luminosity), and we obtain a value of $425h(M_{b,J}/L)_\odot$ for a $10^{15}h^{-1}M_\odot$ halo. For low mass haloes, the resulting mass luminosity relation is dependent on what waveband we are considering, but scaled luminosity goes as $L \sim M^a$ with a roughly between 4 and 4.5 for haloes or subhaloes in the mass range $10^9h^{-1}M_\odot$ to $10^{10}h^{-1}M_\odot$; for example, in the K-band used for our base model, $a \simeq 4.5$. We also find that the occupation number, which can be derived almost directly from the subhalo mass function, scales as $M^{0.9}$.

Finally, we should also make a note on the applicability of the relation we obtained. First, we should stress that this is an average relation. As can be seen from the plotted observational data, we expect a rather large scatter around it. While we feel that obtaining this average relation is quite an important first step and by itself already allows a range of applications, it is important to obtain a model for the scatter if it is to be applied, for example, to build mock catalogues from simulation results. In this direction, there has already been some work on applying the base framework that we have developed further here to a context of a conditional luminosity function, including potential prescriptions for scatter (see work by Cooray and collaborators, e.g. Cooray 2005b; Cooray & Cen 2005). Nonetheless, we feel it is relevant to have a good analysis of the basic framework, especially since the overall simplicity of the model makes it conceptually clear and pedagogical, while at the same time allowing a good comprehension of the factors influencing it.

ACKNOWLEDGEMENTS

We would like to thank George Efstathiou, Ofer Lahav and Edwin Turner for useful comments and suggestions. AV acknowledges financial support from Fundação para a Ciência e Tecnologia (Portugal), under grant SFRH/BD/2989/2000.

REFERENCES

- Abazajian K. et al., 2005, ApJ, 625, 613
- Babul A., Rees M. J., 1992, MNRAS, 255, 346
- Bahcall N. A., Cen R., Davé R., Ostriker J. P., Yu Q., 2000, ApJ, 541, 1
- Bahcall N. A., Ostriker J. P., Perlmutter S., Steinhardt P. J., 1999, Sci, 284, 1481
- Bailin J., et al., 2005, ApJ, 627, L17
- Bell E.F., McIntosh D.H., Katz N., Weinberg M.D., 2003, ApJS, 149, 289
- Benson A. J., 2001, MNRAS, 325, 1039
- Benson A. J., Baugh C. M., Cole S., Frenk C. S., Lacey C. G., 2000a, MNRAS, 316, 107
- Benson A. J., Cole S., Frenk C. S., Baugh C. M., Lacey C. G., 2000b, MNRAS, 311, 793

- Benson A. J., Frenk C. S., Baugh C. M., Cole S., Lacey C. G., 2003, *MNRAS*, 343, 679
- Berlind A. A., Weinberg D. H., 2002, *ApJ*, 575, 587
- Berlind A. A. et al., 2003, *ApJ*, 593, 1
- Bernstein J.P., Bhavsar S.P., 2000, *MNRAS*
- Blanton M. R., et al., 2003, *ApJ*, 592, 819
- Blanton M.R., Lupton R.H., Schlegel D.J., Strauss M.A., Brinkmann J, Fukugita M., Loveday J., 2005, *ApJ*, 631, 208
- Bryan G.L., Norman M., 1998, *ApJ*, 495, 80
- Bullock J. S., Kolatt T. S., Sigad Y., Somerville R. S., Kravtsov A. V., Klypin A. A., Primack J. R., Dekel A., 2001, *MNRAS*, 321, 559
- Bullock J. S., Wechsler R. H., Somerville R. S., 2002, *MNRAS*, 329, 246
- Cole S., Lacey C.G., Baugh C.M., Frenk C.S., 2000, *MNRAS*, 319, 168
- Colless M., 1989, *MNRAS*, 237, 799
- Cooray A., 2005a, *MNRAS*, 363, 337
- Cooray A., 2005b, *astro-ph/0509033*, submitted to *MNRAS*
- Cooray A., Cen R., 2005, *astro-ph/0506423*, submitted to *ApJ*
- Cooray A., Milosavljević M., 2005a, *ApJ*, 627, L85
- Cooray A., Milosavljević M., 2005b, *ApJ*, 627, L89
- Croton D. J. et al., 2005, *MNRAS*, 356, 1155
- De Lucia G., et al., 2004, *MNRAS*, 348, 333
- Dekel A., 2004, *astro-ph/0401503*
- Dekel A., Birnboim Y., 2004, *astro-ph/0412300*, submitted to *ApJ*
- Dekel A., Woo J., 2003, *MNRAS*, 344, 1131
- Eisenstein D.J. et al., 2001, *AJ*, 122, 2267
- Eke V.R. et al., 2004, *MNRAS*, 355, 769
- Eke V.R., Baugh C.M., Cole S., Frenk C.S., Navarro J.F., 2005, *astro-ph/0510643*, submitted to *MNRAS*
- Fukugita M., Hogan C. J., Peebles P. J. E., 1998, *ApJ*, 503, 518
- Gao L., White S.D.M., Jenkins A., Stoehr F., Springel V., 2004, *MNRAS*, 355, 819
- Governato F., Baugh C. M., Frenk C. S., Cole S., Lacey C. G., Quinn T., Stadel J., 1998, *Natur*, 392, 359
- Hayashi E., Navarro J. F., Taylor J. E., Stadel J., Quinn T., 2003, *ApJ*, 584, 541
- Hoekstra H., Yee H. K. C., Gladders M. D., 2002, *ApJ*, 577, 595
- Jarrett T.H., Chester T., Cutri R., Schneider S., Skrutskie M., Huchra J.P., 2000, *AJ*, 119, 2498
- Kauffmann G., White S.D.M., Guiderdoni B., 1993, *MNRAS*, 264, 201
- Kauffmann G., Colberg J. M., Diaferio A., White S. D. M., 1999a, *MNRAS*, 303, 188
- Kauffmann G., Colberg J. M., Diaferio A., White S. D. M., 1999b, *MNRAS*, 307, 529
- Kravtsov A. V., Berlind A. A., Wechsler R. H., Klypin A. A., Gottlöber A., Allgood B., Primack J. R., 2004, *ApJ*, 2004, 609, 35
- Kauffmann G., Nusser A., Steinmetz M., 1997, *MNRAS*, 286, 795
- Kochanek C. S., et al., 2001, *ApJ*, 560, 566
- Kochanek C. S., White M., Huchra J., Macri L., Jarrett T. H., Schneider S. E., Mader J., 2003, *ApJ*, 585, 161
- Libeskind N.I., Frenk C.S., Cole S., Helly J.C., Jenkins A., Navarro J.F., Power C., 2005, *MNRAS*, 363, 146
- Lin Y., Mohr J.J., 2004, *ApJ*, 610, 745
- Lin Y., Mohr J.J., Stanford S.A., 2004, *ApJ*, *astro-ph/0402308*
- Magliocchetti M., Porciani C., 2003, *MNRAS*, 346, 186
- Mateo M. L., 1998, *ARA&A*, 36, 435
- Marinoni C., Hudson M. J., Giuricin G., 2002, *ApJ*, 569, 91
- Meza A., Navarro J.F., Steinmetz M., Eke V.R., 2003, *ApJ*, 590, 619
- Mobasher B., Trentham N., 1998, *MNRAS*, 293, 315
- Moore B., Frenk C. S., White S. D. M., 1993, *MNRAS*, 261, 827
- Nagamine K., Fukugita M., Cen R., Ostriker J. P., 2001, *ApJ*, 558, 497
- Navarro J. F., Frenk C. S., White S. D. M., 1997, *ApJ*, 490, 493
- Norberg P. et al., 2002, *MNRAS*, 336, 907
- Oguri M. & Lee J., 2004, *ApJ*, 355, 120
- Peacock J. A., Smith R. E., 2000, *MNRAS*, 318, 1144
- Pearce F. R., Jenkins A., Frenk C. S., White S. D. M., Thomas P. A., Couchman H. M. P., Peacock J. A., Efstathiou G., 2001, *MNRAS*, 326, 649
- Popesso P., Böhringer H., Brinkmann J., Voges W., York D.G., 2004, *A&A*, 423, 449
- Sanchez A.G., Baugh C.M., Percival W.J., Padilla N.D., Cole S., Frenk C.S., Norberg P., 2005, *astro-ph/0507583*, submitted to *MNRAS*
- Schechter P., 1976, *ApJ*, 203, 297
- Seljak U., 2000, *MNRAS*, 318, 203
- Shaw L., Weller J., Ostriker J.P., Bode P., 2005, *astro-ph/0509856*, submitted to *ApJ*
- Sheth R. K., Diaferio A., 2001, *MNRAS*, 322, 901
- Sheth R. K., Tormen G., *MNRAS*, 1999, 308, 119
- Somerville R.S., Primack J.R., 1999, *MNRAS*, 310, 1087
- Somerville R. S., Lemson G., Sigad Y., Dekel A., Kauffmann G., White S. D. M., 2001, *MNRAS*, 320, 289
- Spergel D. N. et al., 2003, *ApJS*, 148, 175
- Tasitsiomi A., Kravtsov A.V., Wechsler R.H., Primack J.R., 2004, *ApJ*, 614, 533
- Tegmark M. et al., 2004, *PhysRevD*, 69, 3501
- Thoul A. A., Weinberg D. H., 1996, *ApJ*, 465, 608
- Trentham N., Tully R. B., 2002, *MNRAS*, 335, 712
- Trentham N., Sampson L., Banerji M., 2005, *MNRAS*, 357, 783
- Vale A., Ostriker J. P., 2004, *MNRAS*, 353, 189 (Paper I)
- van den Bosch F. C., Tormen G., Giocoli C., 2005, *MNRAS*, 359, 1029
- van den Bosch F. C., Yang X. H., Mo H.J., 2003, *MNRAS*, 340, 771
- van den Bosch F. C., Yang X., Mo H. J., Norberg P., 2005, *MNRAS*, 356, 1233
- Wechsler R. H., Somerville R. S., Bullock J. S., Kolatt T. S., Primack J. R., Blumenthal G. R., Dekel A., 2001, *ApJ*, 554, 85
- Weller J., Ostriker J. P., Bode P., Shaw L., 2004, *astro-ph/0405445*, submitted to *MNRAS*
- White M., Hernquist L., Springel V., 2001, *ApJ*, 550, L129
- Yang X.H., Mo H.J., Kauffmann G., Chu Y.Q., 2003, *MNRAS*, 339, 387
- Yang X. H., Mo H. J., van den Bosch F. C., 2003, *MNRAS*, 339, 1057

- Yang X., Mo H.J., Jing Y.P., van den Bosch F.C., 2005, MNRAS, 358, 217
- Yoshikawa K., Taruya A., Jing Y. P., Suto Y., 2001, ApJ, 558, 520
- Zehavi I. et al., 2005, ApJ, 630, 1
- Zentner A.R., Berlind A.A., Bullock J.S., Kravtsov A.V., Wechsler R.H., 2005, astro-ph/0411586, submitted to ApJ
- Zheng Z., Tinker J. L., Weinberg D. H., Berlind A. A., 2002, ApJ, 575, 617
- Zheng Z. et al., 2004, astro-ph/0408564